

Three-Dimensional Growth Rate Modeling and Simulation of Silicon Carbide Thermal Oxidation

Vito Šimonka*, Andreas Hössinger[‡], Josef Weinbub*, and Siegfried Selberherr[†]

*Christian Doppler Laboratory for High Performance TCAD at the

[†]Institute for Microelectronics, TU Wien, Gußhausstraße 27-29/E360, 1040 Wien, Austria

[‡]Silvaco Europe Ltd., Compass Point, St Ives, Cambridge, PE27 5JL, United Kingdom

Email: simonka@iue.tuwien.ac.at

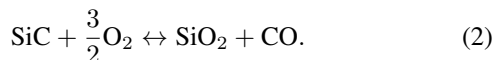
Abstract—We investigate the anisotropic behavior of dry and wet thermal oxidation of silicon carbide for which a high-accuracy three-dimensional simulation model is entirely missing. To bridge this gap, we propose a direction dependent interpolation method for computing oxidation growth rates for three-dimensional problems. We use our method together with available one-dimensional oxidation models to simulate three-dimensional crystal orientation dependent 4H- and 6H-SiC oxidation processes.

I. INTRODUCTION

Silicon carbide (SiC) possesses excellent physical properties for applications in electronic devices operating under high power, high frequency, and high temperature [1]. One of the major advantages of SiC over other wide band gap semiconductors is the ability to thermally oxidize to SiO₂, which has led to the development of SiC power metal-oxide-semiconductor field-effect transistors [2]. Therefore, SiC is a replacement material for silicon (Si), because improving performance of Si power devices can no longer be expected. The devices have reached their performance limit due to the physical properties of Si [3], [4]. Thermal oxidation of Si



is considerably less complicated than the oxidation of SiC



Consequently, thermal oxidation of SiC includes more rate-controlling steps (Fig. 1) [5]–[7]:

- 1) transport of molecular oxygen gas to the oxide surface,
- 2) in-diffusion of oxygen through the oxide film,
- 3) reaction with SiC at the SiO₂/SiC interface,
- 4) out-diffusion of product gases through the oxide film,
- 5) removal of product gases away from the oxide surface.

The last two steps are not involved in the oxidation of Si.

A model for Si oxidation was first introduced by Deal and Grove [8], which suggests that the oxide thickness X is expressed as

$$\frac{dX}{dt} = \frac{B}{A + 2X}, \quad (3)$$

where B/A and B are the linear rate constant and the parabolic rate constant, respectively. B/A is proportional to the reaction

constant of the oxidation process and B is proportional to the diffusion constant of the oxygen through the SiO₂. For thin oxide layers ($2X \ll A$) the limiting step of the oxidation process is the reaction between silicon and oxygen at the Si/SiO₂ interface and for thick oxide layers ($2X \gg A$) the limiting step of the oxidation process is the diffusion of oxygen through the oxide layer.

In the case of SiC, the out-diffusion of product gases plays a significant role in the rate of oxidation. Song *et al.* have proposed a modified Deal-Grove model [2] to describe SiC oxidation kinetics, but rather more accurate is the modified SiC model [3], [9] derived from Massoud's empirical relation [10]–[12]. This model includes an additional exponential term,

$$\frac{dX}{dt} = \frac{B}{A + 2X} + C \exp\left(-\frac{X}{L}\right), \quad (4)$$

where C and L are the exponential prefactor and the characteristic length, respectively. C is proportional to the initial growth rate enhancement and L is proportional to the emission ratios of Si and C, the oxidation coefficient, and the diffusion coefficient of SiO₂ interstitials [3]. For thin oxide layers ($2X \ll A$) or short oxidation times, Eq. 4 can be written as

$$\frac{dX}{dt} \approx \frac{B}{A} + C \exp\left(-\frac{X}{L}\right), \quad (5)$$

where the limiting step of the oxidation process is the interface reaction. For thick oxide layers ($2X \gg A$) or long oxidation times, Eq. 4 can be approximated by

$$\frac{dX}{dt} \approx \frac{B}{2X} + C \exp\left(-\frac{X}{L}\right), \quad (6)$$

where the limiting step of the oxidation process is the diffusion of Si, C, and O₂ through the oxide film.

Massoud's empirical relation can reproduce the oxide growth better than the Deal-Grove model [13], [14]. However, both models are one-dimensional and are not capable of correctly predicting the oxide growth for three-dimensional (3D) SiC structures. Our approach enables accurate 3D modeling by incorporating the crystal direction dependence into the growth rates of the oxidation models.

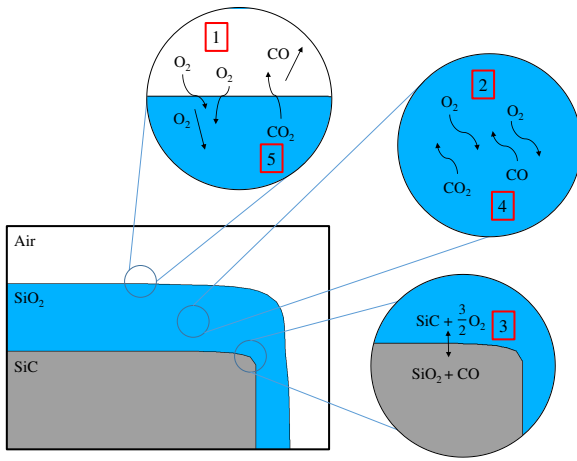


Fig. 1: Schematic representation of thermal oxidation process steps of SiC. 1. Solution of oxygen in the SiO₂, 2. diffusion process of oxygen through the SiO₂, 3. reaction between SiC and O₂ at the SiC/SiO₂ interface, 4. diffusion process of product gases through the SiO₂ and 5. removal of product gases away from the SiO₂.

II. METHOD

The dependence of the oxidation rates on crystal orientation has significant consequences for a non-planar device structure, e.g., the trench design of a U-groove MOSFET, where the oxide is located on all crystallographic planes [15]. The hexagonal structure of SiC gives a large variation in the oxidation rates among different crystal faces [3], [16]. Therefore, we propose an interpolation method to obtain oxidation rates for arbitrary crystal directions according to four known growth rate values.

We have derived a function, which follows the geometry of the hexagonal structure of a crystal and returns a value in the range from 0 to 1 in 3D space

$$f(x, y, z) = \left(2(x^2 + y^2)^3 - (x^2 + y^2)^4 - x^2(x^2 - 3y^2)^2 + z^2 \right) \quad (7)$$

x , y , and z are the crystal direction vector coordinates. The vector $\vec{v}(x, y, z)$ must be normalized, therefore the vector length $|\vec{v}| = 1$. In this case, we can convert Eq. 7 into an interpolation method

$$k(x, y, z) = k_y + \left(k_x - k_y \right) \left(2(x^2 + y^2)^3 - (x^2 + y^2)^4 - x^2(x^2 - 3y^2)^2 \right) + \left(k_z - k_y \right) z^2 \quad (8)$$

where k_x , k_y , and k_z are fixed growth rates in directions of x -, y -, and z -axis, respectively.

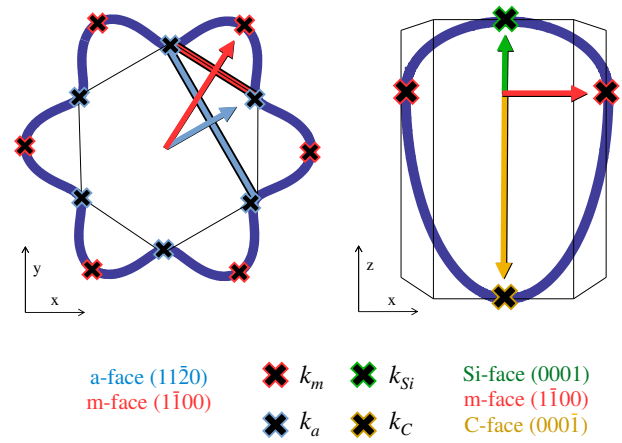


Fig. 2: Schematic illustration of the proposed interpolation method in the x - y (left) and x - z plane (right). The interpolation (dark blue line) is calculated according to the four known growth rate values (black crosses) of Si- (green), m- (red), a- (blue), and C-face (orange square). Colored arrows represent crystal direction vectors towards the corresponding faces. The arrows lengths are proportional to the oxidation growth rates.

Oxidation of SiC is a face-terminated oxidation, i.e., the Si- and the C- face have different oxidation rates [17], therefore we calculate the positive and negative z values separately. The input for the interpolation method are four known growth rate values in the (0001), (1-100), (11-20), and (000-1) directions, which correspond to the Si-, m-, a-, and C-face, respectively, and have been examined experimentally [3], [9], [18]. The proposed 3D interpolation method of the oxidation growth rates is thus

$$k(x, y, z) = k_a + \left(k_m - k_a \right) \left(2(x^2 + y^2)^3 - (x^2 + y^2)^4 - x^2(x^2 - 3y^2)^2 \right) + \left(k_{Si} - k_a \right) z^2 \text{ for } z \geq 0, + \left(k_C - k_a \right) z^2 \text{ for } z < 0, \quad (9)$$

where x , y , and z are crystal direction vector coordinates and k_{Si} , k_m , k_a , and k_C four fixed growth rate values.

The interpolation method follows the same geometrical properties as the parametric method we have proposed recently [19], [20]. It consists of a symmetric star shape in the x - y plane and a tangent-continuous union of two half-ellipses in z direction (Fig. 2). Therefore, both proposed methods match with the hexagonal geometry of SiC, which yields a symmetry in the x - y plane such that the crystal direction from the origin of the crystal (0, 0, 0) towards the a- and m-faces repeat six times with an enclosed angle of $\pi/6$.

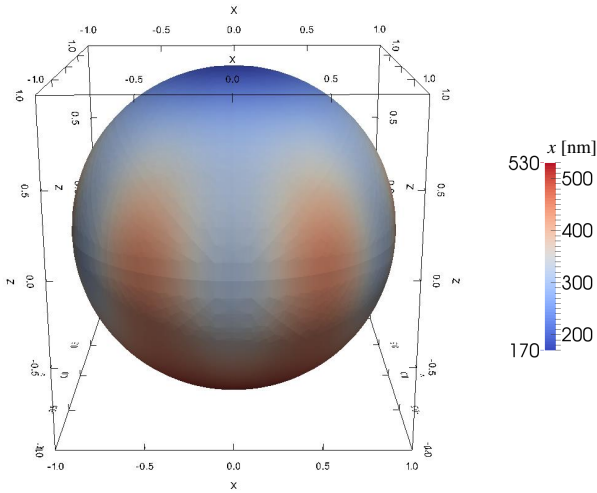


Fig. 3: A sphere of SiC oxide thicknesses obtained with the proposed interpolation method, where the color represents calculated thicknesses towards corresponding crystal directions. The simulations were performed for wet thermal oxidation of 6H-SiC (0001) Si-face (n-type, on-axis) at $T = 1100^\circ\text{C}$ for 720 min.

III. RESULTS

We have performed several 3D calculations of growth rates and simulations of dry and wet thermal oxidation of 4H- and 6H-SiC using the proposed 3D interpolation method and Massoud's empirical relation [10]. We have obtained the fixed growth rate constants B/A , B , $B/A + C$, and L for dry oxidation of (0001) Si-, $(11\bar{2}0)$ a-, and $(000\bar{1})$ C-face 4H-SiC from Goto *et al.* [3]. The growth rate for the $(1\bar{1}00)$ m-face was approximated according to the ratio between the final oxide thicknesses on different crystallographic faces [16]. Growth rates for wet oxidation were obtained from Hosoi *et al.* [21] and our recent study [19].

Fig. 3 shows a sphere of oxide thicknesses for wet thermal oxidation of 6H-SiC. Similar results can be achieved for materials with the same hexagonal crystal structure, e.g., 4H-SiC. The obtained sphere can be directly compared with measurements from Christiansen *et al.* [16]. We also compare the results (Fig. 3) with the results from the parametric interpolation method [19], [20] (Fig. 4). In both simulations as well as in the experimental data we observe star-shape directional dependencies. Moreover, the results are consistent within the numerical and experimental errors.

We have performed simulations of complex 3D structures of dry thermal oxidation of 4H-SiC with Silvaco's Victory Process [22] using the proposed interpolation method. The addition of this method within Victory Process enables to fully simulate arbitrary 3D structures with high precision in oxidation of all crystal directions. Fig. 5 shows the 3D structure of oxidized SiC and Fig. 6 shows two-dimensional cross sections of the 3D simulation. It is obvious that the oxide thickness on the C-face is thickest and the oxide on the Si-face

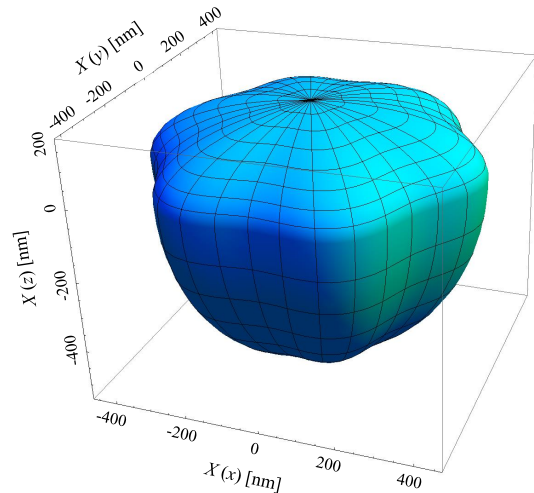


Fig. 4: A 3D simulation of wet thermal oxidation of 6H-SiC at $T = 1100^\circ\text{C}$ for 720 min using the parametric interpolation method [19], [20].

is thinnest. It is harder to see the differences between the m- and a-face, but by careful examination of the data (Fig. 6c), we see that the oxide in the x direction is approximately 10% thicker than the one in the y direction.

IV. CONCLUSIONS

The anisotropy of 4H- and 6H-SiC oxidation processes with regard to the surface orientations was investigated. By carefully studying geometrical aspects of the hexagonal crystal structure, we have proposed an interpolation method to compute oxidation growth rates for 3D problems. The interpolation method includes the well known anisotropy of the oxidation of the Si- and the C-face, as well as the anisotropic behavior of the m- and the a-face. Six maxima and six minima, corresponding to the crystal symmetry in the shape of a star, are computed in the basic crystal plane x - y , which intersects with the origin of the unit cell.

With the proposed interpolation method we have computed oxide thicknesses for wet thermal oxidation of 6H-SiC and compared the results with 3D simulations and experiments from literature. The proposed interpolation method fits the geometry dependence of 4H- and 6H-SiC oxidation very well. Additionally, we have simulated dry thermal oxidation of an arbitrary shape of 4H-SiC with Silvaco's Victory Process using the proposed method. As is to be expected [16], [23], for wet and dry thermal oxidation processes, the grown oxide exhibits different thicknesses in dependence of the crystal directions.

ACKNOWLEDGMENT

The financial support by the *Austrian Federal Ministry of Science, Research and Economy* and the *National Foundation for Research, Technology and Development* is gratefully acknowledged.

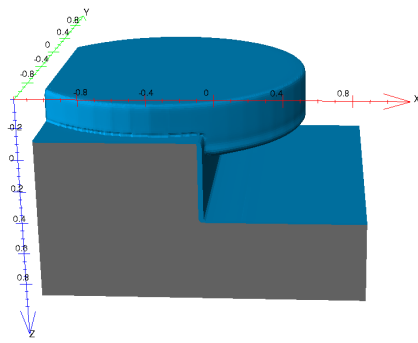


Fig. 5: A 3D simulation of dry thermal oxidation of SiC using the proposed method. The simulation was performed for 4H-SiC (0001) Si-face (n-type, on-axis) at $T = 1100^\circ\text{C}$ for 120 min. Gray areas are 4H-SiC and blue areas represent the grown SiO_2 .

REFERENCES

- [1] J. Casady and R. W. Johnson, *Solid-State Electronics*, vol. 39, no. 10, pp. 1409–1422, 1996.
- [2] Y. Song, S. Dhar, L. C. Feldman, G. Chung, and J. R. Williams, *Journal of Applied Physics*, vol. 95, no. 9, pp. 4953–4957, 2004.
- [3] D. Goto, Y. Hijikata, S. Yagi, and H. Yaguchi, *Journal of Applied Physics*, vol. 117, no. 9, p. 095306, 2015.
- [4] Y. Hijikata. InTech, Croatia, 2013.
- [5] J. Schmitt and R. Helbig, *Journal of The Electrochemical Society*, vol. 141, no. 8, pp. 2262–2265, 1994.
- [6] I. C. Vickridge, J. J. Ganem, G. Battistig, and E. Szilagy, *Nuclear Instruments and Methods in Physics Research Section B: Beam Interactions with Materials and Atoms*, vol. 161, pp. 462–466, 2000.
- [7] J. M. Knaup, P. Deák, T. Frauenheim, A. Gali, Z. Hajnal, and W. J. Choyke, *Physical Review B*, vol. 71, no. 23, p. 235321, 2005.
- [8] B. E. Deal and A. Grove, *Journal of Applied Physics*, vol. 36, no. 12, pp. 3770–3778, 1965.
- [9] Y. Hijikata, H. Yaguchi, and S. Yoshida, *Applied Physics Express*, vol. 2, no. 2, p. 021203, 2009.
- [10] H. Z. Massoud, J. D. Plummer, and E. A. Irene, *Journal of the Electrochemical Society*, vol. 132, no. 7, pp. 1745–1753, 1985.
- [11] H. Z. Massoud, J. D. Plummer, and E. A. Irene, *Journal of the Electrochemical Society*, vol. 132, no. 11, pp. 2685–2693, 1985.
- [12] H. Z. Massoud, J. D. Plummer, and E. A. Irene, *Journal of the Electrochemical Society*, vol. 132, no. 11, pp. 2693–2700, 1985.
- [13] T. Yamamoto, Y. Hijikata, H. Yaguchi, and S. Yoshida, *Japanese Journal of Applied Physics*, vol. 46, no. 8L, p. L770, 2007.
- [14] T. Yamamoto, Y. Hijikata, H. Yaguchi, and S. Yoshida, *Japanese Journal of Applied Physics*, vol. 47, no. 10R, p. 7803, 2008.
- [15] C. Harris and V. Afanas'ev, *Microelectronic Engineering*, vol. 36, no. 1–4, pp. 167–174, 1997.
- [16] K. Christiansen and R. Helbig, *Journal of Applied Physics*, vol. 79, no. 6, pp. 3276–3281, 1996.
- [17] T. Yamamoto, Y. Hijikata, H. Yaguchi, and S. Yoshida, in *Proceedings of Materials Science Forum*, pp. 667–670, 2009.
- [18] J. J. Ahn, Y. D. Jo, S. C. Kim, J. H. Lee, and S. M. Koo, *Nanoscale Research Letters*, vol. 6, no. 1, pp. 1–5, 2011.
- [19] V. Šimonka, G. Nawratil, A. Hössinger, J. Weinbub, and S. Selberherr, *Solid-State Electronics*, 2016, under review.
- [20] V. Šimonka, G. Nawratil, A. Hössinger, J. Weinbub, and S. Selberherr, in *Proceedings of 2016 Joint International EUROSOI Workshop and International Conference on Ultimate Integration on Silicon*, pp. 226–229, 2016.
- [21] T. Hosoi, D. Nagai, T. Shimura, and H. Watanabe, *Japanese Journal of Applied Physics*, vol. 54, no. 9, p. 098002, 2015.
- [22] http://www.silvaco.com/products/tcad/process_simulation/victory_process/victory_process.html.
- [23] N. Tokura, K. Hara, T. Miyajima, H. Fuma, and K. Hara, *Japanese Journal of Applied Physics*, vol. 34, no. 10R, p. 5567, 1995.

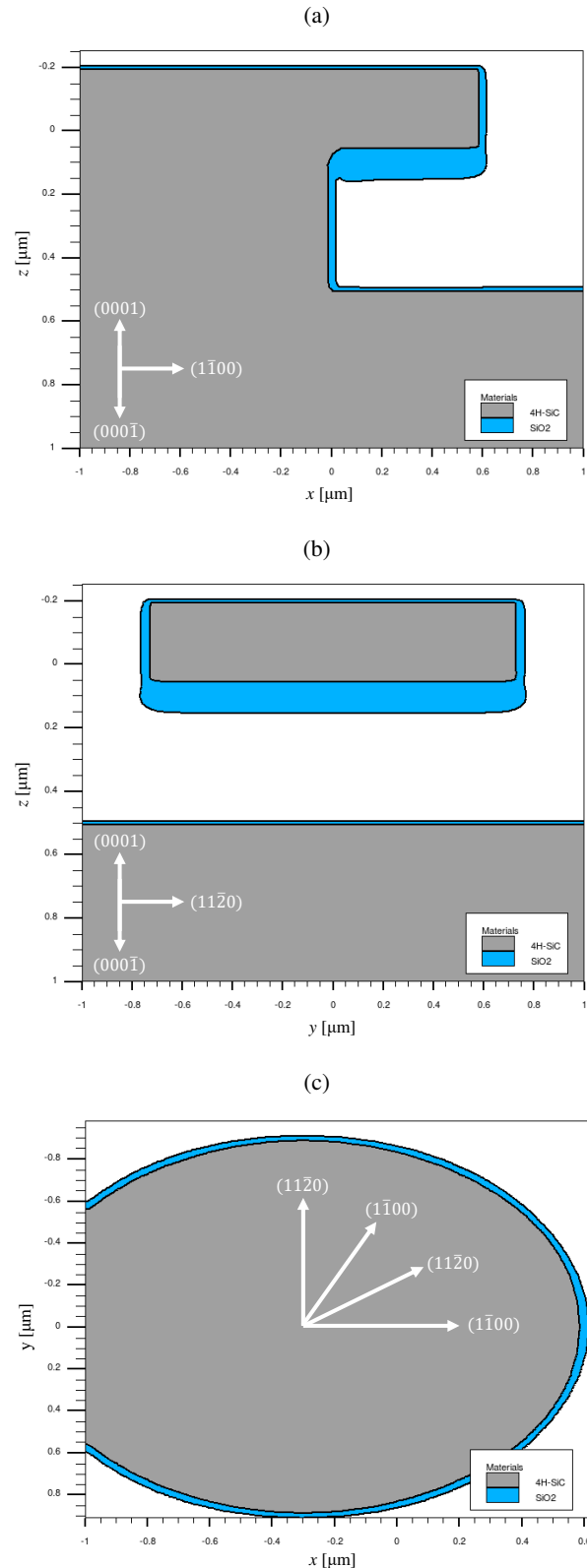


Fig. 6: Two-dimensional cross sections of the conducted 3D simulations of 4H-SiC dry thermal oxidation (Fig. 5). **a)** x - z cross section at $y = 0.0 \mu\text{m}$, **b)** y - z cross section at $x = 0.2 \mu\text{m}$, and **c)** x - y cross section at $z = -0.2 \mu\text{m}$.